

Coulomb Effects in Femtoscopy

Radosław Maj^{*}

Institute of Physics, Jan Kochanowski University, ul. Świętokrzyska 15, PL-25-406 Kielce, Poland

Stanisław Mrówczyński[†]

*Institute of Physics, Jan Kochanowski University, ul. Świętokrzyska 15, PL-25-406 Kielce, Poland
and Soltan Institute for Nuclear Studies, ul. Hoża 69, PL-00-681 Warsaw, Poland*

(Dated: September 28, 2009)

The correlation function of two identical particles - pions or kaons - interacting via Coulomb potential is computed. The particles are emitted from an anisotropic particle's source of finite lifetime. In the case of pions, the effect of halo is taken into account as an additional particle's source of large spatial extension. The relativistic effects are discussed in detail. The Bowler-Sinyukov procedure to remove the Coulomb interaction is carefully tested. In the absence of halo the procedure is shown to work very well even for an extremely anisotropic source. When the halo is taken into account the free correlation function, which is extracted by means of the Bowler-Sinyukov procedure, is distorted at small relative momenta but the source parameters are still correctly reproduced.

PACS numbers: 25.75.-q, 25.75.Gz

I. INTRODUCTION

The correlation functions of two particles with small relative momenta provide information about space-time characteristics of particle's sources in high-energy nucleus-nucleus collisions, see the review articles [1, 2, 3, 4]. Within the standard femtoscopy, one obtains parameters of a particle's source, comparing the experimental correlation functions to the theoretical ones which are calculated in a given model. Such an analysis can be performed for pairs of non-identical or identical particles. In the former case, the correlation appears due to inter-particle interaction while in the latter one the interaction is combined with the effects of quantum statistics. Since we usually deal with electrically charged particles, observed two-particle correlations are strongly influenced by the Coulomb interaction. The effect of the Coulomb force is usually eliminated from experimental data by means of the so-called Bowler-Sinyukov procedure [5, 6]. And then, the correlation function, which is obtained in such a way from experimental data, is compared to the theoretical correlation function of two non-interacting particles. The comparison provides parameters of the source of particles.

The femtoscopy was applied to a large volume of experimental data on nucleus-nucleus collisions at SPS energy as summarized in [7]. The spatial size of particle's sources appeared to be comparable to the expected size a fireball created in nucleus-nucleus collisions while the emission time of particles was significantly shorter. It was predicted that at RHIC energies the emission time would be significantly longer due to the long lasting hydrodynamic evolution of the system created at the early stage of nucleus-nucleus collisions [8, 9]. To a big surprise the experimental data obtained at RHIC [10, 11, 12, 13] show a very little change of the space-time characteristics of a fireball when compared to the SPS data. In particular, the emission time of particles appeared to be as short as 1 fm/c. Because of this surprising result, which is now known as the 'HBT Puzzle' [14, 15], a reliability of the femtoscopy was questioned.

As an alternative to the standard femtoscopy, the method of imaging [16, 17] was developed. Within this method one obtains the source function not referring to its specific parametrization but directly inverting the correlation function. The procedure of inversion takes into account the effect of quantum statistics as well as that of inter-particle interaction. The one-dimensional and three-dimensional imaging was successfully applied to experimental data, see [18, 19] and [20, 21, 22], respectively. The method provides essentially model independent information on the source space-time sizes but modeling is still needed to deduce the emission time which is coupled to spatial parameters of the source. Therefore, the imaging has not much helped to resolve the 'HBT puzzle'.

Very recently it has been shown that hydrodynamic calculations can be modified to give quite short emission times of produced particles [23], see also [24, 25]. Specifically, the initial condition needs to be changed to speed up formation of the transverse collective flow and the first order phase transition from quark-gluon plasma to hadron gas should be replaced by the smooth cross-over. Another solution of the 'HBT Puzzle' assumes an incomplete equilibrium of

* radmaj@ujk.kielce.pl

† mrow@fuw.edu.pl

quark-gluon plasma [26]. Although the ‘HBT Puzzle’ is resolvable now, if not resolved in [23, 24, 25, 26], it is still of interest to quantitatively check the femtoscopy method, to be sure that experimentally obtained source parameters are indeed reliable. This is the aim of our study which is mainly focused on the Coulomb effects. Our preliminary results were presented in [27] but, unfortunately, some errors appeared in this publication.

The Bowler-Sinyukov correction procedure, which is used to eliminate the Coulomb interaction from the experimental data, assumes that the Coulomb effects can be factorized out. The correction’s factor is calculated for a particle’s source which is spherically symmetric and has zero lifetime. We examine the procedure applying it to the computed Coulomb correlation functions of identical particles coming from anisotropic sources of finite lifetime. Azimuthally asymmetric sources, which appear in azimuthally sensitive femtoscopy [28, 29], are also studied. We treat the computed Coulomb correlation functions as experimentalists treat the measured correlation functions. Thus, we extract the correlation function which is supposed to be free of the Coulomb interaction. However, in contrast to the situation of experimentalists we know actual parameters of particle sources which can be compared to the extracted ones. Our analysis is somewhat similar to that presented in [30] where the Coulomb correlation functions were computed by means of Monte Carlo event generator and it was claimed that the procedure of removal of the Coulomb effects works well. Our analysis is more detailed and it is based on mostly analytical calculations.

The correlation function of two identical non-interacting bosons is expected to be equal to 2 for vanishing relative momentum of the two particles. The correlation functions extracted from experimental data by means of the procedure, which is supposed to remove the Coulomb interaction, do not possess this property. The correlation function at zero relative momentum is significantly smaller than 2. This fact is usually explained referring to the concept of halo [31]. It assumes that only a fraction of observed particles comes from the fireball while the rest originates from the long living resonances. Then, we have two sources of particles: the fireball and the halo with the radius given by the distance traveled by long living resonances. The complete correlation function, which includes particles from the fireball and the halo, equals 2 at exactly vanishing relative momentum. However, the correlation of two particles coming from the halo occurs at a relative momentum which is as small as the inverse radius of the halo. Since experimental momentum resolution is usually much poorer and such small relative momenta are not accessible, the correlation function is claimed to be less than 2 for *effectively* vanishing relative momentum. We carefully study the effect of halo and, in particular, we test how the Bowler-Sinyukov correction procedure works in the presence of halo.

We discuss in detail how to compute the Coulomb correlation functions. We pay particular attention to relativistic effects which, in our opinion, are not clearly exposed in literature. We start with the nonrelativistic Koonin formula [32] because of its rather transparent physical meaning. A more formal derivation of the correlation function, which follows the studies [33, 34, 35], is sketched in the Appendix A. The Koonin formula expresses the correlation function through the nonrelativistic wave function of two particles of interest. Since the observed correlation functions are significantly different from unity only for small relative momenta when the relative motion of particles is nonrelativistic, it is legitimate to use the nonrelativistic wave function in the center-of-mass frame of two particles. However, it requires an explicit transformation of the source function to the center-of-mass frame. It should be mentioned that transformation properties of nonrelativistic wave function under a Lorentz boost are not well understood. Only recently it has been shown using the Bethe-Salpeter equation that the hydrogen atom wave function experiences the Lorentz contraction [36] under the Lorentz boost. Therefore, we perform the calculation in the center-of-mass frame of the pair and then we transform the correlation function to the source rest frame.

Throughout our whole analysis the source function is of the Gaussian form. Such a choice has several advantages. First of all, the Gaussian source functions are often used to describe experimental data. Actually, the imaging method [16, 17] shows that non-Gaussian contributions to the source functions are at a percent level [18, 19, 20, 21, 22]. There are also pure theoretical advantages of the Gaussian parameterization. When the single particle source function is Gaussian, the so-called relative source function is Gaussian as well. Since the Gaussian source function has a simple Lorentz covariant form, Lorentz transformations can be easily performed. Due to the two features of the Gaussian source functions, our calculations are mainly analytical which in turn allowed us, in particular, to carefully study relativistic effects mentioned above.

The Gaussian parameterization we use has an important disadvantage - the fireball expansion is entirely neglected. The study of source expansion, however, goes beyond the scope of our analysis. We address in this paper a specific question whether the Bowler-Sinyukov procedure properly removes Coulomb effects from the correlation functions. For this purpose we compute the Coulomb correlation function with the Gaussian source, we apply the Bowler-Sinyukov procedure and we check how accurately the free correlation function, which is also computed with the Gaussian source, is reproduced. It is certainly of interest to study how the fireball’s expansion influences the Coulomb effects. Before that, however, one should systematically analyze to what extent the expanding fireball can be represented by a Gaussian source. For this reason we do not discuss the interplay of Coulomb interaction and fireball expansion. Actually, the problem cannot be addressed using the computational methods we developed.

Throughout the paper we use natural units, where $c = \hbar = 1$, and our metric convention is $(+, -, -, -)$.

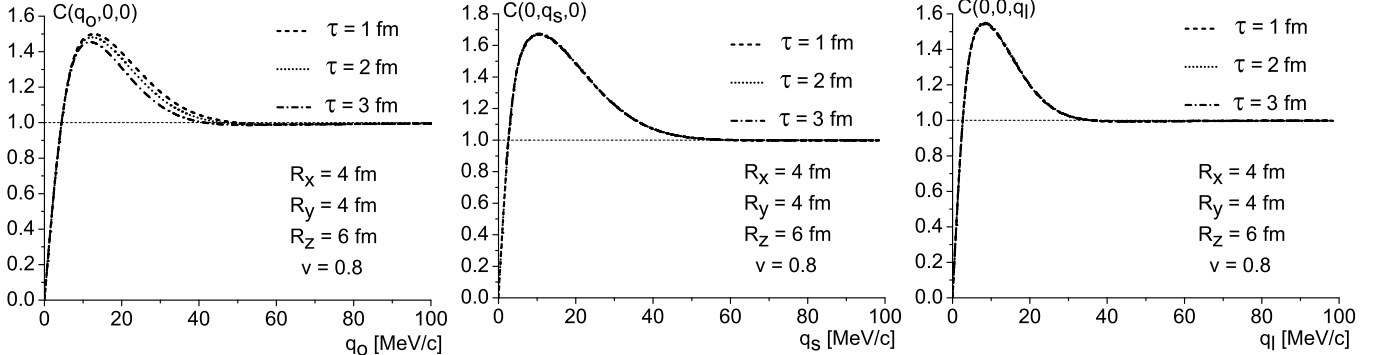


FIG. 1: The $\pi\pi$ Coulomb correlation functions $C(q_0, 0, 0)$ (left panel), $C(0, q_s, 0)$ (central panel) and $C(0, 0, q_i)$ (right panel) as functions of q_0 , q_s or q_i , respectively, for three values of the emission time $\tau = 1, 2, 3$ fm. The remaining parameters are: $R_x = 4$ fm, $R_y = 4$ fm, $R_z = 6$ fm, and $v = (0.8, 0, 0)$.

II. DEFINITION

The correlation function $C(\mathbf{p}_1, \mathbf{p}_2)$ of two particles with momenta \mathbf{p}_1 and \mathbf{p}_2 is defined as

$$C(\mathbf{p}_1, \mathbf{p}_2) = \frac{\frac{dN}{d\mathbf{p}_1 d\mathbf{p}_2}}{\frac{dN}{d\mathbf{p}_1} \frac{dN}{d\mathbf{p}_2}}, \quad (1)$$

where $\frac{dN}{d\mathbf{p}_1 d\mathbf{p}_2}$ and $\frac{dN}{d\mathbf{p}_1}$ is, respectively, the two- and one-particle momentum distribution. The correlation function can be written down in a Lorentz covariant form

$$C(\mathbf{p}_1, \mathbf{p}_2) = \frac{E_1 E_2 \frac{dN}{d\mathbf{p}_1 d\mathbf{p}_2}}{E_1 \frac{dN}{d\mathbf{p}_1} E_2 \frac{dN}{d\mathbf{p}_2}}, \quad (2)$$

where $E \frac{dN}{d^3 p}$ is the Lorentz invariant distribution.

The covariant form (2) shows that the correlation function is a Lorentz scalar field which can be easily transformed from one reference frame to another. If the particle four-momenta, which are on mass-shell, transform as $\mathbf{p}_i \rightarrow \mathbf{p}'_i$ with $i = 1, 2$, the transformed correlation function equals

$$C'(\mathbf{p}'_1(\mathbf{p}_1), \mathbf{p}'_2(\mathbf{p}_2)) = C(\mathbf{p}_1, \mathbf{p}_2).$$

III. NONRELATIVISTIC KOONIN FORMULA

Within the Koonin model [32], the correlation function C can be expressed in the source rest frame as

$$C(\mathbf{p}_1, \mathbf{p}_2) = \int d^3 r_1 dt_1 d^3 r_2 dt_2 D(t_1, \mathbf{r}_1) D(t_2, \mathbf{r}_2) |\Psi(\mathbf{r}'_1, \mathbf{r}'_2)|^2, \quad (3)$$

where $\mathbf{r}'_i \equiv \mathbf{r}_i + \mathbf{v}_i t_i$, $\Psi(\mathbf{r}'_1, \mathbf{r}'_2)$ is the wave function of the two particles and $D(t, \mathbf{r})$ is the single-particle source function which gives the probability to emit the particle from the space-time point (t, \mathbf{r}) . The source function is normalized as

$$\int d^3 r dt D(t, \mathbf{r}) = 1. \quad (4)$$

After changing the variables $\mathbf{r}' \leftrightarrow \mathbf{r}$, the correlation function can be written in the form

$$C(\mathbf{p}_1, \mathbf{p}_2) = \int d^3 r_1 dt_1 d^3 r_2 dt_2 D(t_1, \mathbf{r}_1 - \mathbf{v}_1 t_1) D(t_2, \mathbf{r}_2 - \mathbf{v}_2 t_2) |\Psi(\mathbf{r}_1, \mathbf{r}_2)|^2.$$

Now, we introduce the center-of-mass coordinates

$$\begin{aligned} \mathbf{r} &= \mathbf{r}_2 - \mathbf{r}_1, & \mathbf{R} &= \frac{1}{M}(m_1 \mathbf{r}_1 + m_2 \mathbf{r}_2), \\ t &= t_2 - t_1, & T &= \frac{1}{M}(m_1 t_1 + m_2 t_2), \\ \mathbf{q} &= \frac{1}{M}(m_2 \mathbf{p}_1 - m_1 \mathbf{p}_2), & \mathbf{P} &= \mathbf{p}_1 + \mathbf{p}_2, \end{aligned}$$

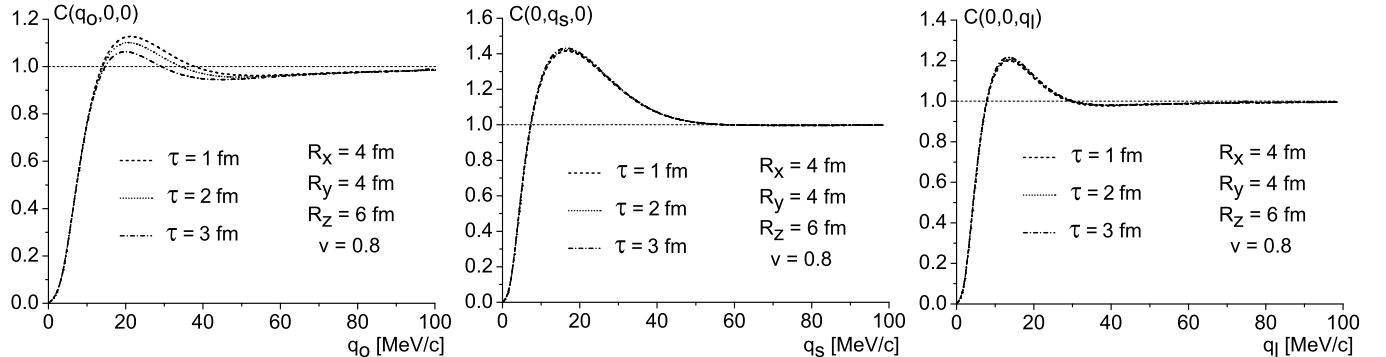


FIG. 2: The KK Coulomb correlation functions $C(q_o, 0, 0)$ (left panel), $C(0, q_s, 0)$ (central panel) and $C(0, 0, q_l)$ (right panel) as functions of q_o , q_s or q_l , respectively, for three values of the emission time $\tau = 1, 2, 3$ fm. The remaining parameters are: $R_x = 4$ fm, $R_y = 4$ fm, $R_z = 6$ fm, and $\mathbf{v} = (0.8, 0, 0)$.

where $M \equiv m_1 + m_2$. Using the center-of-mass variables, one gets

$$C(\mathbf{q}) = \int d^3r D_r(\mathbf{r}) |\varphi_{\mathbf{q}}(\mathbf{r})|^2, \quad (5)$$

where the ‘effective relative’ source function is defined as

$$D_r(\mathbf{r}) \equiv \int dt D_r(t, \mathbf{r} - \mathbf{v}t), \quad (6)$$

and the ‘relative’ source function is expressed through the single-particle source function in the following way

$$D_r(t, \mathbf{r}) \equiv \int d^3R dT D(T - \frac{m_2}{M}t, \mathbf{R} - \frac{m_2}{M}\mathbf{r}) D(T + \frac{m_1}{M}t, \mathbf{R} + \frac{m_1}{M}\mathbf{r}). \quad (7)$$

We note that due to the normalization (4), the functions $D_r(\mathbf{r})$ and $D_r(\mathbf{r} - \mathbf{v}t, t)$ are also normalized

$$\int d^3r D_r(\mathbf{r}) = \int d^3r dt D_r(t, \mathbf{r}) = 1. \quad (8)$$

To get Eq. (5), the wave function was factorized as

$$\Psi(\mathbf{r}_1, \mathbf{r}_2) = e^{i\mathbf{P}\mathbf{R}} \varphi_{\mathbf{q}}(\mathbf{r})$$

with $\varphi_{\mathbf{q}}(\mathbf{r})$ being the wave function of the relative motion in the center-of-mass frame. Deriving Eq. (5), it has been assumed that the particle velocity, which enters the effective source function, is the same for both particles. Thus, we have assumed that $\mathbf{v}_1 = \mathbf{v}_2 = \mathbf{v}$ which requires, strictly speaking, $\mathbf{q} = 0$. However, one observes that $|\mathbf{v}_1 - \mathbf{v}_2| \ll |\mathbf{v}_i|$ if $|\mathbf{q}| \ll \mu|\mathbf{p}_i|/m_i$ where $\mu \equiv m_1 m_2 / M$. Thus, the approximation $\mathbf{v}_1 \approx \mathbf{v}_2$ holds for sufficiently small particle’s momenta in the center-of-mass frame. It should be stressed that the dependence of the correlation function on \mathbf{q} is mostly controlled by the dependence of the wave function on \mathbf{q} which is not influenced by the above approximation.

We choose the Gaussian form of the single-particle source function $D(t, \mathbf{r})$

$$D(t, \mathbf{r}) = \frac{1}{4\pi^2 R_x R_y R_z \tau} \exp \left[-\frac{t^2}{2\tau^2} - \frac{x^2}{2R_x^2} - \frac{y^2}{2R_y^2} - \frac{z^2}{2R_z^2} \right], \quad (9)$$

where $\mathbf{r} = (x, y, z)$ and the parameters τ , R_x , R_y and R_z characterize the lifetime and sizes of the source. Specifically, the parameters τ and R_x give, respectively,

$$\tau^2 = \langle t^2 \rangle \equiv \int d^3r dt t^2 D(t, \mathbf{r}), \quad R_x^2 = \langle x^2 \rangle \equiv \int d^3r dt x^2 D(t, \mathbf{r}).$$

The relative source function computed from Eq. (7) with the single-particle source (9) is

$$D_r(t, \mathbf{r}) = \frac{1}{16\pi^2 R_x R_y R_z \tau} \exp \left[-\frac{t^2}{4\tau^2} - \frac{x^2}{4R_x^2} - \frac{y^2}{4R_y^2} - \frac{z^2}{4R_z^2} \right]. \quad (10)$$

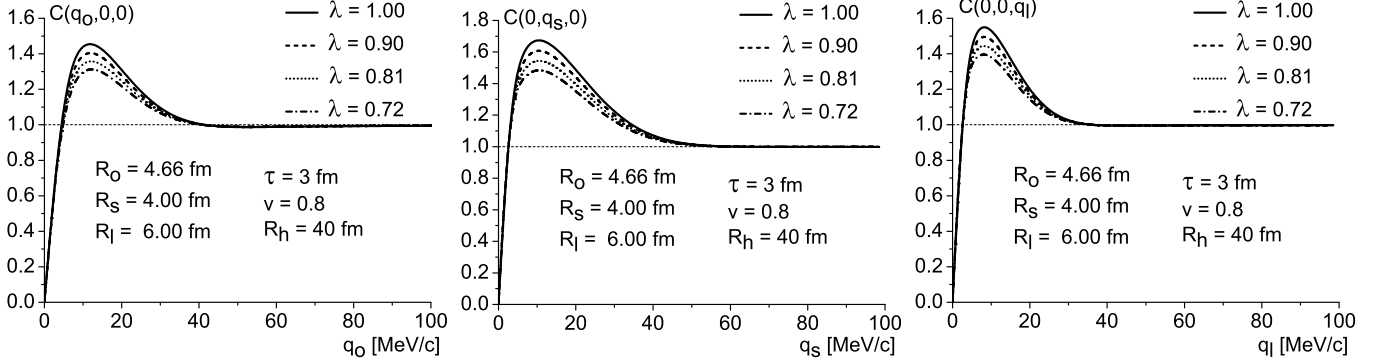


FIG. 3: The $\pi\pi$ Coulomb correlation functions $C(q_o, 0, 0)$ (left panel), $C(0, q_s, 0)$ (central panel) and $C(0, 0, q_l)$ (right panel) as functions of q_o , q_s or q_l , respectively, for various halo contributions. The halo is spherical with $R_h = 40$ fm and $\tau_h = 0$. The fireball parameters are $R_x = 4$ fm, $R_y = 4$ fm, $R_z = 6$ fm, $\tau = 3$ fm. The pair velocity is $v = (0.8, 0, 0)$.

We note that the particle's masses, which are present in the definition (7), disappear completely in the formula (10). This is the feature of the Gaussian parameterization (9).

In the case of non-interacting identical bosons, the two-particle symmetrized wave function is

$$\Psi(\mathbf{r}_1, \mathbf{r}_2) = \frac{1}{\sqrt{2}}[e^{i\mathbf{p}_1\mathbf{r}_1 + i\mathbf{p}_2\mathbf{r}_2} + e^{i\mathbf{p}_2\mathbf{r}_1 + i\mathbf{p}_1\mathbf{r}_2}] = \frac{1}{\sqrt{2}}[e^{i\mathbf{qr}} + e^{-i\mathbf{qr}}]e^{i\mathbf{PR}}.$$

It gives the modulus square of the wave function of relative motion $|\varphi_{\mathbf{q}}(\mathbf{r})|^2 = 1 + \cos(2\mathbf{qr})$ which in turn provides the correlation function equal to

$$C(\mathbf{q}) = 1 + \exp[-4(\tau^2(\mathbf{qv})^2 + R_x^2q_x^2 + R_y^2q_y^2 + R_z^2q_z^2)], \quad (11)$$

where $\mathbf{q} \equiv (q_x, q_y, q_z)$. We note that the ‘cross terms’ such as $q_x q_z$, which are discussed in [37], do not show up, as the source function (9) obeys the mirror symmetry $D(t, \mathbf{r}) = D(-t, -\mathbf{r})$. We also note that \mathbf{q} often denotes the relative momentum $\mathbf{p}_1 - \mathbf{p}_2$ not the momentum in the center-of-mass frame, which for equal mass nonrelativistic particles equals $\frac{1}{2}(\mathbf{p}_1 - \mathbf{p}_2)$, and then, the factor 4 does not show up in the correlation function (11) of identical free bosons. However, we believe that using the momentum in the center-of-mass frame is physically better motivated, as the center-of-mass variables naturally appear when the center-of-mass motion is separated from the relative one.

IV. RELATIVISTIC FORMULATIONS

There are two natural ways to ‘relativize’ the Koonin formula (3). The first one provides an explicitly Lorentz covariant correlation function but it is applicable only for the non-interacting particles. The second one holds only in a specific reference frame but it is applicable for interacting particles as well. Below, we consider the two methods. We start, however, with the discussion of the Lorentz covariant form of the source function.

A. Lorentz covariant source function

Because of its probabilistic interpretation, the source function transforms under Lorentz transformation as a scalar field. Therefore, the covariant form of the Gaussian parameterization of the source function (9) is written as [38]

$$D(x) = \frac{\sqrt{\det \Lambda}}{4\pi^2} \exp[-\frac{1}{2}x_\mu \Lambda^{\mu\nu} x_\nu], \quad (12)$$

where x^μ is the position four-vector and $\Lambda^{\mu\nu}$ is the Lorentz tensor characterizing the source which in the source rest frame is

$$\Lambda^{\mu\nu} = \begin{bmatrix} \frac{1}{\tau^2} & 0 & 0 & 0 \\ 0 & \frac{1}{R_x^2} & 0 & 0 \\ 0 & 0 & \frac{1}{R_y^2} & 0 \\ 0 & 0 & 0 & \frac{1}{R_z^2} \end{bmatrix}. \quad (13)$$

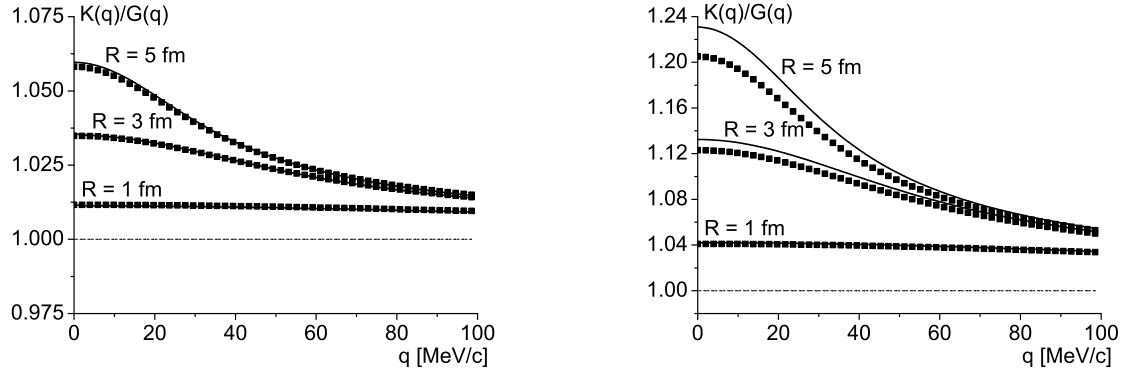


FIG. 4: The correction factor $K(q)$ divided by the Gamov factor $G(q)$ as function of q for source radii $R = 1, 3, 5$ fm. The left panel is for pions and the right one for kaons. The solid lines and squares represent, respectively, the exact formula (35) and the approximate one (36).

The source function as written in Eq. (12) obeys the normalization condition (4) not only for the diagonal matrix Λ but for non-diagonal as well.

The source function (12) is evidently the Lorentz scalar that is

$$D'(x') = \frac{\sqrt{\det\Lambda'}}{4\pi^2} \exp\left[-\frac{1}{2}x'_\mu\Lambda'^{\mu\nu}x'_\nu\right] = \frac{\sqrt{\det\Lambda}}{4\pi^2} \exp\left[-\frac{1}{2}x_\mu\Lambda^{\mu\nu}x_\nu\right] = D(x), \quad (14)$$

where $x'_\mu = L_\mu^\nu x_\nu$ and $\Lambda'^{\mu\nu} = L_\sigma^\mu \Lambda^{\sigma\rho} L_\rho^\nu$ with L_σ^μ being the matrix of Lorentz transformation. We note that $\det\Lambda' = \det L \det\Lambda \det L^{-1} = \det\Lambda$.

The covariant relative source function (10) is given by

$$D_r(x) = \frac{\sqrt{\det\Lambda}}{16\pi^2} \exp\left[-\frac{1}{4}x_\mu\Lambda^{\mu\nu}x_\nu\right]. \quad (15)$$

B. Explicitly covariant ‘relativization’

As follows from Eq. (2), the correlation function is a Lorentz scalar. Therefore, the Koonin formula (3) can be ‘relativized’ demanding its Lorentz covariance. Let us write the formula as

$$C(p_1, p_2) = \int d^4x_1 d^4x_2 D(x_1) D(x_2) |\Psi(x_1, x_2)|^2, \quad (16)$$

where p_i and x_i is, respectively, the four-momentum and four-position. Since the source function $D(x)$ and the four-volume element d^4x_i are both the Lorentz scalars, the whole formula (16) is covariant if the wave function $\Psi(x_1, x_2)$ is covariant as well. In the case of non-interacting bosons the relativistic wave function $\Psi(x_1, x_2)$ is

$$\Psi(x_1, x_2) = \frac{1}{\sqrt{2}}(e^{ip_1 x_1 + ip_2 x_2} + e^{ip_1 x_2 + ip_2 x_1}). \quad (17)$$

As the function depends on the scalar products of two four-vectors, it is the Lorentz scalar. We note that the function (17) depends on two time arguments.

Our further considerations are limited to pairs of identical particles and thus, we introduce the relative coordinates:

$$\begin{aligned} x &= x_2 - x_1, & X &= \frac{1}{2}(x_1 + x_2), \\ q &= \frac{1}{2}(p_1 - p_2), & P &= p_1 + p_2. \end{aligned} \quad (18)$$

In this section and in Appendix A q is the four-vector (q_0, \mathbf{q}) but in the remaining sections $q \equiv |\mathbf{q}|$. Hopefully, it will not cause any confusion.

We note that in the nonrelativistic treatment the three-vectors \mathbf{r} and \mathbf{q} , which are given by the four-vectors $x = (t, \mathbf{r})$ and $q = (q_0, \mathbf{q})$, correspond to the inter-particle separation and the particle’s momentum in the center-of-mass of the

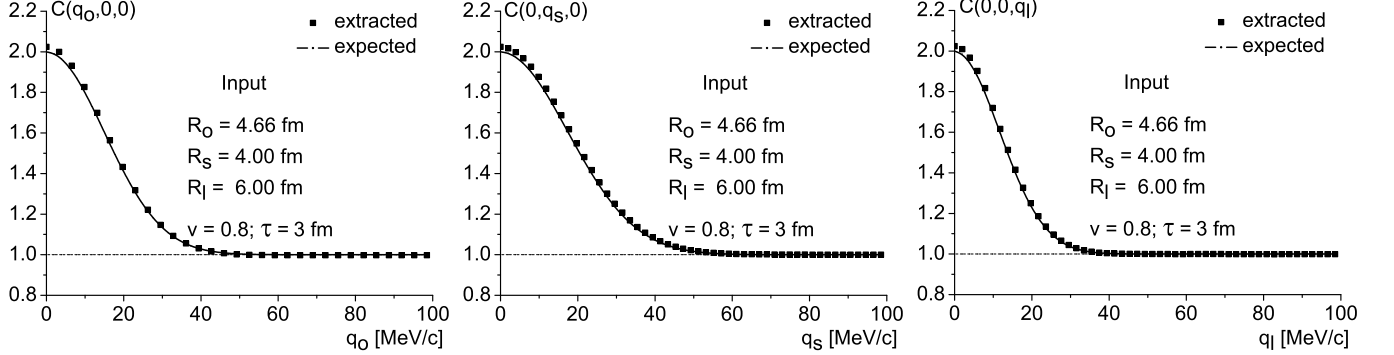


FIG. 5: The $\pi\pi$ free correlation functions $C(q_0, 0, 0)$ (left panel), $C(0, q_s, 0)$ (central panel) and $C(0, 0, q_i)$ (right panel) as a function of q_0 , q_s or q_i , respectively. The fireball parameters are $R_x = 4$ fm, $R_y = 4$ fm, $R_z = 6$ fm, $\tau = 3$ fm and the pair velocity is $\mathbf{v} = (0.8, 0, 0)$. The extracted ‘free’ functions are represented by the squares and the expected free correlation functions by the solid lines.

pair. This is, however, not the case in the relativistic domain. To get the center-of-mass variables, the four-vectors need to be Lorentz transformed. We also note that $q_0 = \mathbf{q}\mathbf{v}$ which is proven as [45]

$$q_0 \equiv \frac{1}{2} \left(\sqrt{m^2 + \mathbf{p}_1^2} - \sqrt{m^2 + \mathbf{p}_2^2} \right) = \frac{1}{2} \frac{\mathbf{p}_1^2 - \mathbf{p}_2^2}{\sqrt{m^2 + \mathbf{p}_1^2} + \sqrt{m^2 + \mathbf{p}_2^2}} = \mathbf{q} \frac{\mathbf{p}_1 + \mathbf{p}_2}{\sqrt{m^2 + \mathbf{p}_1^2} + \sqrt{m^2 + \mathbf{p}_2^2}} = \mathbf{q}\mathbf{v} .$$

With the variables (18), the wave function (17) equals

$$\Psi(x, X) = \frac{1}{\sqrt{2}} (e^{iqx} + e^{-iqx}) e^{iPX} ,$$

and the correlation function is found in the form

$$C(q) = 1 + \exp[-4q_\mu(\Lambda^{\mu\nu})^{-1}q_\nu] ,$$

which is explicitly Lorentz covariant. For the source matrix (13), the correlation function equals

$$C(q) = 1 + \exp[-4(q_0^2\tau^2 + q_x^2R_x^2 + q_y^2R_y^2 + q_z^2R_z^2)] . \quad (19)$$

Since $q_0 = \mathbf{q}\mathbf{v}$, the correlation function (19) exactly coincides with the nonrelativistic expression (11). This coincidence is not completely obvious as the time variables enter differently in the Koonin formula (3) and in the covariant one (16).

Let us consider the correlation function in the center-of-mass frame of the particle pair. We assume that the velocity of the center-of-mass frame in the source rest frame is along the axis x . Then, $\mathbf{v} = (v, 0, 0)$ and $q_0 = q_x v$. The correlation function (19), which holds in the source rest frame, equals

$$C(\mathbf{q}) = 1 + \exp[-4((v^2\tau^2 + R_x^2)q_x^2 + R_y^2q_y^2 + R_z^2q_z^2)] . \quad (20)$$

As seen, the effective source radius in the direction x is $\sqrt{R_x^2 + v^2\tau^2}$. We now transform the source function to the center-of-mass frame where the quantities are labeled with the index $*$. The center-of-mass source matrix (13), which is computed as

$$\Lambda_*^{\mu\nu} = L^\mu_{\sigma} \Lambda^{\sigma\rho} L_\rho^{\nu} ,$$

where

$$L^\mu_{\sigma} = \begin{bmatrix} \gamma & -v\gamma & 0 & 0 \\ -v\gamma & \gamma & 0 & 0 \\ 0 & 0 & 1 & 0 \\ 0 & 0 & 0 & 1 \end{bmatrix}$$

with $\gamma \equiv (1 - v^2)^{-1/2}$, equals

$$\Lambda_*^{\mu\nu} = \begin{bmatrix} \gamma^2(\frac{1}{\tau^2} + \frac{v^2}{R_x^2}) & -\gamma^2 v(\frac{1}{\tau^2} + \frac{1}{R_x^2}) & 0 & 0 \\ -\gamma^2 v(\frac{1}{\tau^2} + \frac{1}{R_x^2}) & \gamma^2(\frac{v^2}{\tau^2} + \frac{1}{R_x^2}) & 0 & 0 \\ 0 & 0 & \frac{1}{R_y^2} & 0 \\ 0 & 0 & 0 & \frac{1}{R_z^2} \end{bmatrix} . \quad (21)$$

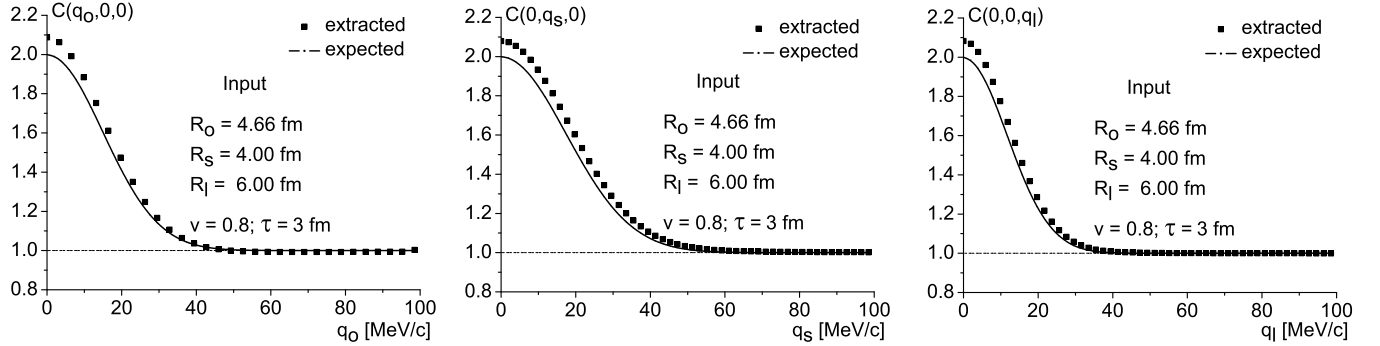


FIG. 6: The KK free correlation function $C(q_o, 0, 0)$ (left panel), $C(0, q_s, 0)$ (central panel) and $C(0, 0, q_l)$ (right panel) as a function of q_o , q_s or q_l , respectively. The fireball parameters are $R_x = 4$ fm, $R_y = 4$ fm, $R_z = 6$ fm, $\tau = 3$ fm and the pair velocity is $\mathbf{v} = (0.8, 0, 0)$. The extracted ‘free’ functions are represented by the squares and the expected free correlation functions by the solid lines.

Then, the correlation function in the center-of-mass frame is found to be

$$C(q_*) = 1 + \exp[-4q_{*\mu}(\Lambda_*^{\mu\nu})^{-1}q_{*\nu}] = 1 + \exp[-4(\gamma^2(v^2\tau^2 + R_x^2)q_{*x}^2 + R_y^2q_{*y}^2 + R_z^2q_{*z}^2)]. \quad (22)$$

As seen, the effective source radius along the direction of the velocity is elongated, not contracted as one can naively expect, by the factor γ .

C. Non-covariant relativization

The quantum mechanical description of two relativistic interacting particles faces serious difficulties. The problem is greatly simplified when the relative motion of two particles is nonrelativistic (with the center-of-mass motion being fully relativistic). Since the correlation functions usually differ from unity only for small relative momenta of particles, it is reasonable to assume that the relative motion is nonrelativistic. We further discuss the correlation functions taking into account the relativistic effects of motion of particles with respect to the source but the particle’s relative motion is treated nonrelativistically. In such a case, the wave function of relative motion is a solution of the nonrelativistic Schrödinger equation. Thus, we compute the correlation function directly from the Koonin formula (3) but the computation is performed in the center-of-mass frame of the pair. For this reason we first transform the source function to this frame and then, after performing the integrations over x_1 and x_2 , we transform the whole correlation function to the source rest frame. We stress here that according to the definition (2) the correlation function is the Lorentz scalar.

As already noted, we compute the correlation function in the center-of-mass frame of the pair using the relative variables (18). The correlation function thus equals

$$C(\mathbf{q}_*) = \int d^3r_* dt_* D_r(t_*, \mathbf{r}_*) |\varphi_{\mathbf{q}_*}(\mathbf{r}_*)|^2, \quad (23)$$

where $D_r(t_*, \mathbf{r}_*)$ is the relative source function (15) and $\varphi_{\mathbf{q}_*}(\mathbf{r}_*)$ is, as previously, the nonrelativistic wave function of relative motion. The note here that $\mathbf{v}_* = 0$ by definition. The formula (23) can be rewritten as

$$C(\mathbf{q}_*) = \int d^3r_* D_r(\mathbf{r}_*) |\varphi_{\mathbf{q}_*}(\mathbf{r}_*)|^2, \quad (24)$$

where

$$D_r(\mathbf{r}_*) \equiv \int dt_* D_r(t_*, \mathbf{r}_*) = \frac{1}{8\pi^{3/2}\sqrt{\gamma^2(R_x^2 + v^2\tau^2)R_yR_z}} \exp\left[-\frac{1}{4}\left(\frac{x_*^2}{\gamma^2(R_x^2 + v^2\tau^2)} + \frac{y_*^2}{R_y^2} + \frac{z_*^2}{R_z^2}\right)\right] \quad (25)$$

for $\mathbf{v} = (v, 0, 0)$. One easily checks that the free correlation function, which follows from Eq. (23) or Eq. (24), exactly coincides with the formula (22). To get the correlation function in the source rest frame, one performs the Lorentz transformation (the correlation function as defined by Eq. (2) is a Lorentz scalar) and obtains the formula (20). Thus, the two ways of ‘relativization’ give the same result for non-interacting particles. This is not quite trivial as the time

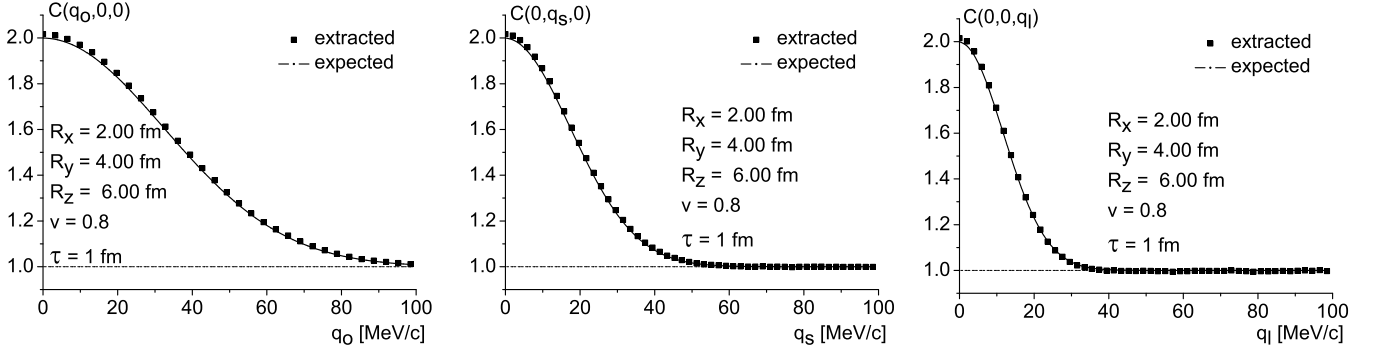


FIG. 7: The $\pi\pi$ Coulomb correlation functions $C(q_o, 0, 0)$ (left panel), $C(0, q_s, 0)$ (central panel) and $C(0, 0, q_l)$ (right panel) as functions of q_o , q_s or q_l , respectively, for the azimuthally asymmetric source. The parameters are: $R_x = 2$ fm, $R_y = 4$ fm, $R_z = 6$ fm, $\tau = 1$ fm and the pair velocity is $\mathbf{v} = (0.8, 0, 0)$. The extracted ‘free’ functions are represented by the squares while the expected free correlation functions correspond to the solid lines.

dependence of the Koonin formula (23) and of the explicitly covariant one (16) look rather different. Unfortunately, we do not know whether the equivalence of the two ‘relativization’ schemes holds for interacting particles, as the covariant ‘relativization’ is known only for free particles.

V. COULOMB CORRELATION FUNCTIONS

In this section we compute, using Eq. (24), the correlation functions of pairs of identical pions or kaons interacting due to the Coulomb force. The calculations are performed for the anisotropic Gaussian source of finite emission time (12, 13). We use the Bertsch-Pratt coordinates [41, 42] *out, side, long*. These are the Cartesian coordinates, where the direction *long* is chosen along the beam axis (z), the *out* is parallel to the component of the pair momentum \mathbf{P} which is transverse to the beam. The last direction - *side* - is along the vector product of the *out* and *long* versors. So, the vector \mathbf{q} is decomposed into the q_o , q_s , and q_l components. If the particle’s velocity is chosen along the axis x , the *out* direction coincides with the direction x , the *side* direction with y and the *long* direction with z . We note that the correlation function of two identical free bosons in the Bertsch-Pratt coordinates in the source rest frame is

$$C(\mathbf{q}) = 1 + \exp \left[-4(q_o^2 R_o^2 + q_s^2 R_s^2 + q_l^2 R_l^2) \right],$$

where $R_o = \sqrt{R_x^2 + v^2 \tau^2}$, $R_s = R_y$ and $R_l = R_z$. As seen, the source lifetime τ is mixed up with the size parameter R_x . Although experimentalists usually use the parameters R_o , R_s , R_l , we use them together with R_x , R_y , R_z and τ , as the lifetime τ naturally enters theoretical formulas. Since the velocity of the pair is chosen along the axis x , we always have $R_s = R_y$ and $R_l = R_z$.

The effect of Coulomb interaction in femtoscopy can be treated analytically or almost analytically under some simplifying approximations [43]. However, we are interested in the exact Coulomb correlation functions. Therefore, we use the exact wave function. In the case of two non-identical particles interacting due to repulsive Coulomb force, the nonrelativistic wave function is well known to be [39]

$$\varphi_{\mathbf{q}}(\mathbf{r}) = e^{-\frac{\pi\eta}{2q}} \Gamma(1 + i\frac{\eta}{q}) e^{i\mathbf{qr}} {}_1F_1 \left(-i\frac{\eta}{q}, 1, i(qr - \mathbf{qr}) \right), \quad (26)$$

where $q \equiv |\mathbf{q}|$ and η^{-1} is the Bohr radius which for pairs of pions and kaons equals $\eta_\pi^{-1} = 388$ fm and $\eta_K^{-1} = 110$ fm, respectively; ${}_1F_1$ denotes the hypergeometric confluent function. When one deals with identical bosons, the wave function $\varphi_{\mathbf{q}}(\mathbf{r})$ should be symmetrized and the modulus of the symmetrized Coulomb wave function equals

$$\begin{aligned} |\varphi_{\mathbf{q}}(\mathbf{r})|^2 &= \frac{1}{2} G(q) \left[|{}_1F_1(-i\frac{\eta}{q}, 1, i(qr - \mathbf{qr}))|^2 + |{}_1F_1(-i\frac{\eta}{q}, 1, i(qr + \mathbf{qr}))|^2 \right. \\ &\quad \left. + 2\text{Re} \left(e^{2i\mathbf{qr}} {}_1F_1(-i\frac{\eta}{q}, 1, i(qr - \mathbf{qr})) {}_1F_1^*(-i\frac{\eta}{q}, 1, i(qr + \mathbf{qr})) \right) \right], \end{aligned} \quad (27)$$

where $G(q)$ is the so-called Gamov factor defined as

$$G(q) = \frac{2\pi\eta}{q} \frac{1}{\exp(\frac{2\pi\eta}{q}) - 1}. \quad (28)$$

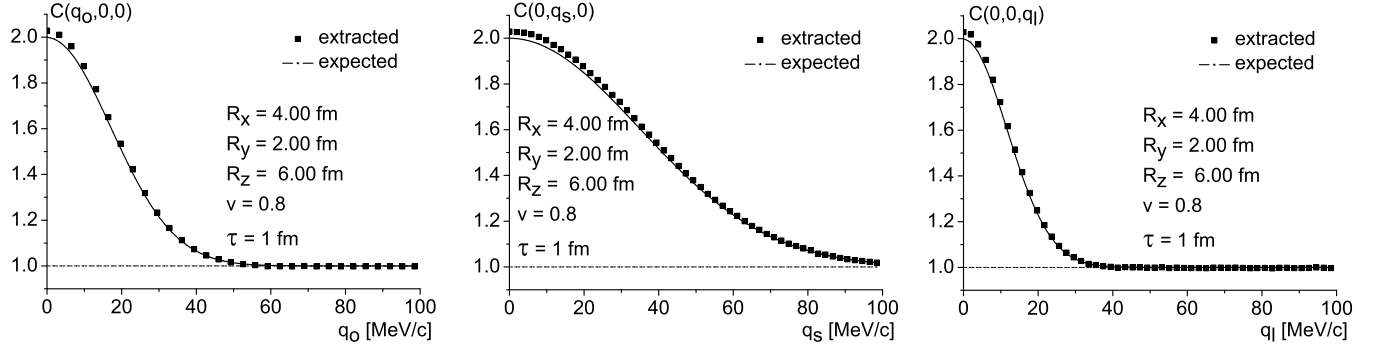


FIG. 8: The $\pi\pi$ Coulomb correlation functions $C(q_o, 0, 0)$ (left panel), $C(0, q_s, 0)$ (central panel) and $C(0, 0, q_l)$ (right panel) as functions of q_o , q_s or q_l , respectively, for the azimuthally asymmetric source. The parameters are: $R_x = 4 \text{ fm}$, $R_y = 2 \text{ fm}$, $R_z = 6 \text{ fm}$, $\tau = 1 \text{ fm}$ and the pair velocity is $v = (0.8, 0, 0)$. The extracted ‘free’ functions are represented by the squares while the expected free correlation functions correspond to the solid lines.

One may wonder whether a multi-particle environment, which occurs in the final state of relativistic heavy-ion collisions, influences the Coulomb potential of the two particles of interest. It should be remembered, however, that the particles are correlated at small relative momenta and thus, they fly with similar velocities. Consequently, after the time comparable to the source size, the particles with small relative velocity appear to be effectively isolated from the rest of many-particle system. Therefore, the effect of screening of Coulomb potential is expected to be negligible. This qualitative argument is confirmed by the calculations presented in [40].

Substituting the modulus (27) and the source function (25) into Eq. (24), one finds the correlation function in the center-of-mass frame which is further transformed to the source rest frame. In Figs. 1 and 2 we show the correlation functions $C(q_o, 0, 0)$, $C(0, q_s, 0)$ and $C(0, 0, q_l)$ of identical pions and kaons, respectively. The calculations are performed for the following values of the source parameters: $R_x = 4 \text{ fm}$, $R_y = 4 \text{ fm}$, $R_z = 6 \text{ fm}$, and $\tau = 1, 2, 3 \text{ fm}$. The velocity of the particle’s pair with respect to the source equals $v = 0.8$ and it is along the axis x . As seen, the correlation functions of pions and kaons differ sizably due to the different Bohr radii of the two systems. The most visible difference appears for the function $C(q_o, 0, 0)$.

VI. THE HALO

As mentioned in the introduction, the halo [31] was introduced to explain the fact that, after removing the Coulomb effect, the experimentally measured correlation functions are smaller than 2 at vanishing relative momentum. The idea of halo assumes that only a fraction f ($0 \leq f \leq 1$) of particles contributing to the correlation function comes from the fireball or core while the remaining fraction ($1 - f$) originates from long living resonances. Then, we have two sources of the particles: the small one - the fireball or core - and the big one corresponding to the long living resonances. The single-particle source function has two contributions

$$D(t, \mathbf{r}) = f D_f(t, \mathbf{r}) + (1 - f) D_h(t, \mathbf{r}), \quad (29)$$

where $D_f(t, \mathbf{r})$ and $D_h(t, \mathbf{r})$ represent the fireball and halo, respectively. For non-interacting identical bosons, the correlation function is

$$C(\mathbf{q}) = 1 + f^2 e^{-4R_f^2 \mathbf{q}^2} + (1 - f)^2 e^{-4R_h^2 \mathbf{q}^2} + 2f(1 - f)e^{-2(R_f^2 + R_h^2)\mathbf{q}^2}, \quad (30)$$

where both the fireball and halo are assumed to be spherically symmetric sources of zero lifetimes; R_f and R_h are the radii of, respectively, the fireball and the halo. If R_h is so large that R_h^{-1} is below an experimental resolution of the relative momentum \mathbf{q} , the third and fourth term of the correlation function (30) are effectively not seen, and one claims that $C(\mathbf{q} = 0) = 1 + \lambda$ with $\lambda \equiv f^2 < 1$.

We have included the halo in our calculations of the $\pi\pi$ Coulomb correlation functions. Since the halo represents pions from resonances, the source function of the halo, which was carefully modeled in [44], is approximately of the exponential form. In our calculations, however, the halo source function, as other source functions we use, is of the Gaussian form for the reasons explained in the introduction. Our simplified treatment of the halo seems to be harmless, as the halo influences the correlation function only for q of the order R_h^{-1} which are experimentally hardly accessible.

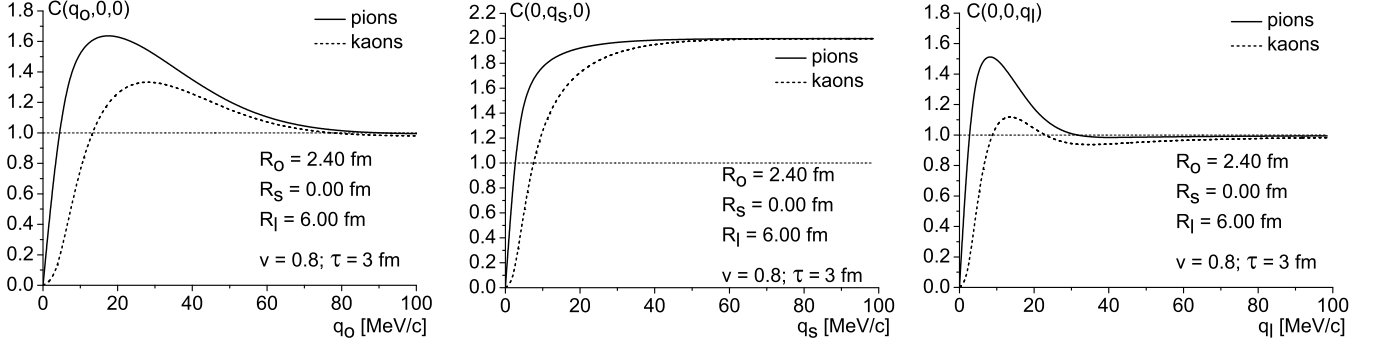


FIG. 9: The $\pi\pi$ and KK Coulomb correlation functions $C(q_o, 0, 0)$ (left panel), $C(0, q_s, 0)$ (central panel) and $C(0, 0, q_l)$ (right panel) as functions of q_o , q_s or q_l , respectively, for the extremely anisotropic source. The parameters are $R_x = R_y = 0$, $R_z = 6$ fm, $\tau = 3$ fm and the pair velocity is $v = (0.8, 0, 0)$.

Our exemplary results are shown in Figs. 3 for several values of λ . The fireball is anisotropic with $R_x = 4$ fm, $R_y = 4$ fm, $R_z = 6$ fm, $\tau = 3$ fm and $v = 0.8$; the halo is spherically symmetric, its radius is $R_h = 40$ fm (as suggested in [31]) and its lifetime vanishes.

In principle, a finite spatial extension of the halo implies a finite duration of pion emission. However, when the finite lifetime of the halo is taken into account, the size of the halo in the out direction increases, and the correlation function observed in this direction is influenced at even smaller momenta than those in the side and long directions. In other words, neglecting the finite lifetime of the halo, its effect on the correlation function in the out direction is overestimated not underestimated. We return to this point at the end of Sec. X.

VII. COULOMB CORRECTION WITHOUT HALO

As mentioned in the Introduction, the Coulomb effect is usually subtracted from the experimentally measured correlation functions by means of the Bowler-Sinyukov procedure. We first note that the Coulomb effect is far not small and thus the method to subtract the Coulomb effect should be carefully tested.

In the absence of halo the Bowler-Sinyukov procedure assumes that the Coulomb effect can be factorized out, that is the correlation function can be expressed as

$$C(\mathbf{q}) = K(q) C_{\text{free}}(\mathbf{q}), \quad (31)$$

where $C_{\text{free}}(\mathbf{q})$ is the free correlation function and $K(q)$ is the correction factor which can be treated as the Coulomb correlation function of two nonidentical particles of equal masses and charges. The function is, however, rather unphysical as the pair velocity vanishes even so the calculation is performed in the rest frame of the source where the source is assumed to be symmetric and of zero lifetime. The correction factor $K(q)$, which is described in detail in the Appendix to the paper [30], is computed as

$$K(q) = G(q) \int d^3r D_r(\mathbf{r}) |{}_1F_1(-\frac{i\eta}{q}, 1, iq(r - \mathbf{qr}))|^2, \quad (32)$$

where $G(q)$ is the Gamov factor (28) and $D_r(\mathbf{r})$ describes the spherically symmetric Gaussian source of zero lifetime and of the ‘effective’ radius $R = \sqrt{(R_o^2 + R_s^2 + R_l^2)/3}$ where $R_o = \sqrt{R_x^2 + v^2\tau^2}$, $R_s = R_y$ and $R_l = R_z$ are the femtoscopic radii obtained from the extracted free correlation function. Experimentally R_o , R_s and R_l are found fitting the measured correlation function $C(\mathbf{q})$ with $K(q) C_{\text{free}}(\mathbf{q})$. In our theoretical analysis, R_x , R_y , R_z and τ are the actual source parameters which enter the source function (9).

Using the parabolic coordinates $\xi_+ \equiv r + z$, $\xi_- \equiv r - z$ and the azimuthal angle ϕ , the relative source function of isotropic Gaussian source of zero lifetime is

$$D_r(\xi_+, \xi_-, \phi) = \frac{1}{8\pi^{3/2}R^3} \exp\left(-\frac{(\xi_+ + \xi_-)^2}{16R^2}\right), \quad (33)$$

which substituted into Eq. (32) gives

$$K(q) = \frac{G(q)}{16\pi^{1/2}R^3} \int_0^\infty d\xi_+ \int_0^\infty d\xi_- (\xi_+ + \xi_-) \left| {}_1F_1\left(-\frac{i\eta}{q}, 1, iq\xi_-\right) \right|^2 \exp\left(-\frac{(\xi_+ + \xi_-)^2}{16R^2}\right). \quad (34)$$

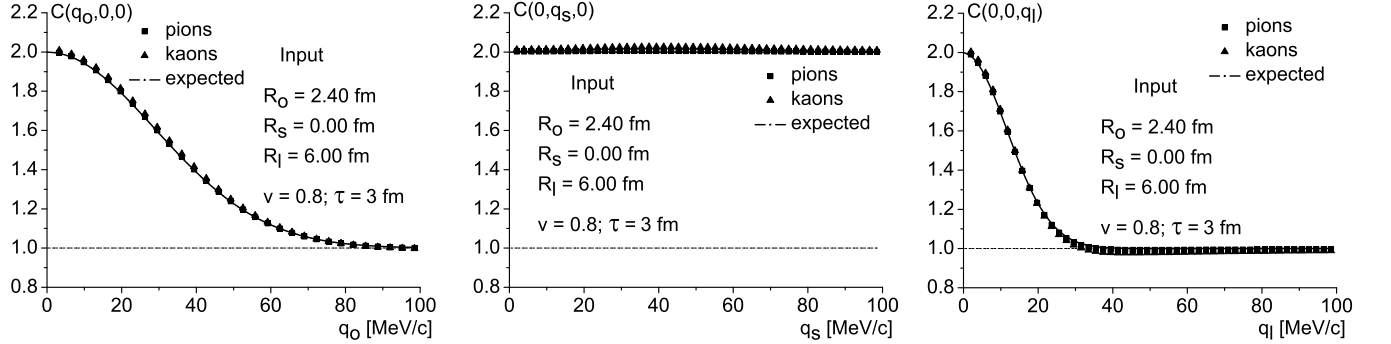


FIG. 10: The $\pi\pi$ and KK ‘free’ correlation functions $C(q_o, 0, 0)$ (left panel), $C(0, q_s, 0)$ (central panel) and $C(0, 0, q_l)$ (right panel) as functions of q_o , q_s or q_l , respectively, for the extremely anisotropic source. The parameters are: $R_x = R_y = 0$, $R_z = 6$ fm, $\tau = 3$ fm and the pair velocity is $\mathbf{v} = (0.8, 0, 0)$. The extracted ‘free’ functions are represented by the squares for pions and by triangles for kaons; the expected free correlation functions correspond to the solid lines.

The trivial integral over ϕ has been performed in Eq. (34). Since the confluent hypergeometric function does not depend on ξ_+ , the integral over ξ_+ can be easily performed and one obtains

$$K(q) = \frac{G(q)}{2\pi^{1/2}R} \int_0^\infty d\xi_- \left| {}_1F_1\left(-\frac{i\eta}{q}, 1, iq\xi_-\right) \right|^2 \exp\left(-\frac{\xi_-^2}{16R^2}\right), \quad (35)$$

where the integral over ξ_- is usually computed numerically. However, observing that the source size is always much smaller than the Bohr radius of the particles of interest, one derives the approximate expression of the hyperbolic confluent function (B9) which is discussed in Appendix B. With the formula (B10) the integration can be performed analytically and the correction factor equals

$$K(q) = G(q) \left[1 + \frac{8\eta R}{\sqrt{\pi}} {}_2F_2\left(\frac{1}{2}, 1; \frac{3}{2}, \frac{3}{2}; -4q^2R^2\right) \right]. \quad (36)$$

In Fig. 4 we show the correction factor $K(q)$ for pions and kaons computed from the exact formula (32) and the approximate one (36). To make the difference more visible (note the vertical scale) the correction factor is divided by the Gamov factor which strongly varies with q . One sees that the approximation (36) is very accurate for pions and it is less accurate for kaons. For this reason the expression (36) is used only for pions. Fig. 4 also shows that the correction factor is heavily dominated by the Gamov factor that is $K(q)/G(q)$ differs very little from unity.

Once we are able to compute the exact Coulomb correlation functions for an anisotropic source of finite lifetime, we can test whether the free correlation function obtained by means of the Bowler-Sinyukov equation (31) properly reproduces the actual free correlation function.

The free correlation functions, which are obtained using Eq. (31), are shown in Fig. 5 for pions in Fig. 6 for kaons. The extracted functions are compared to the expected correlation functions of noninteracting bosons for the given source. As seen, the free correlation function is almost exactly reproduced in the case of pions while in the case of kaons the reproduction is less accurate. Similar results are found as long as the source radii are much smaller than the Bohr radius of particles of interest.

VIII. AZIMUTHALLY SENSITIVE FEMTOSCOPY

In the previous sections we discussed the particle sources of cylindrical (azimuthal) symmetry ($R_x = R_y$). The sources created in non-central collisions are not azimuthally symmetric but the symmetry is usually restored due to the averaging over impact parameter orientation. The cylindrically asymmetric sources are observable, if the reaction plane is determined. The azimuthally sensitive femtoscopy was developed [28, 29] and when applied to experimental data it showed an expected dependence of the source radii on the emission angle with respect to the reaction plane. Since the Coulomb effects were removed from the data by means of the Bowler-Sinyukov procedure in the experimental studies [28, 29], we test in this section the procedure for the case azimuthally asymmetric sources.

We do not study a full dependence of the correlation function on the azimuthal emission angle but we consider two extreme cases. We stick to our convention that particles are always emitted along the axis x but $R_x \neq R_y$. In Fig. 7 we show the pion correlation functions $C(q_o, 0, 0)$, $C(0, q_s, 0)$ and $C(0, 0, q_l)$ for $R_x = 2$ fm, $R_y = 4$ fm and in Fig. 8

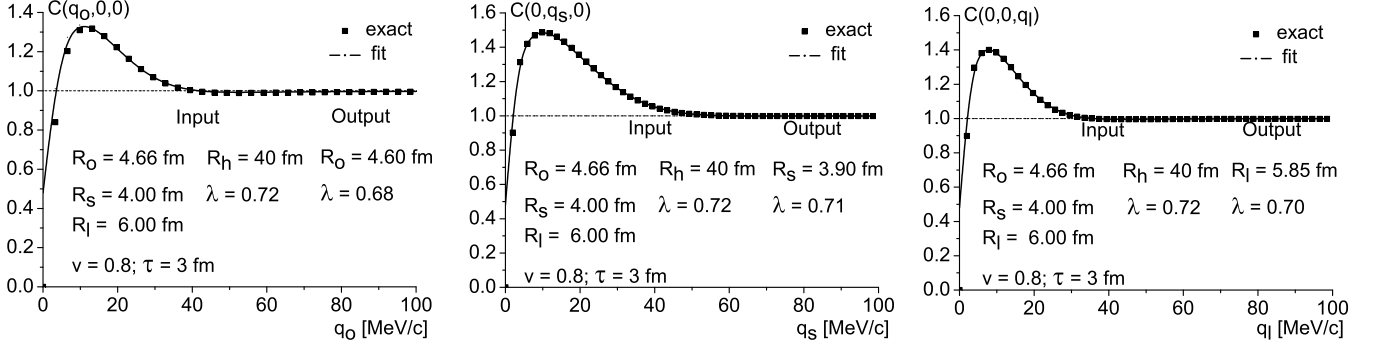


FIG. 11: The $\pi\pi$ Coulomb correlation functions $C(q_o, 0, 0)$ (left panel), $C(0, q_s, 0)$ (central panel) and $C(0, 0, q_l)$ (right panel) as functions of q_o , q_s or q_l , respectively. The fireball and halo parameters are $R_x = 4$ fm, $R_y = 4$ fm, $R_z = 6$ fm, $\tau = 3$ fm, $R_h = 40$ fm and the pair velocity is $\mathbf{v} = (0.8, 0, 0)$. The exact Coulomb correlation functions are shown with the squares and the Coulomb correlation functions fitted with the dilution formula (41) are represented by the solid lines.

the case $R_x = 4$ fm, $R_y = 2$ fm is illustrated. The remaining parameters are $R_z = 6$ fm, $\tau = 1$ fm, $\mathbf{v} = (0.8, 0, 0)$. As seen, the Bowler-Sinyukov procedure works very well in both cases.

IX. EXTREMELY ANISOTROPIC SOURCE

To establish limitations of the Bowler-Sinyukov procedure in the absence of halo, we have considered an extremely anisotropic source where R_z is much larger than R_x and R_y as well as $R_z \gg \tau$. The source function is found from Eq. (25) by taking the limits $R_y \rightarrow 0$, $R_x \rightarrow 0$ and $\tau \rightarrow 0$. Thus, one finds

$$D_r(\mathbf{r}_*) = \frac{1}{2\pi^{1/2}R_z} \exp\left[-\frac{z_*^2}{4R_z^2}\right] \delta(x_*)\delta(y_*) . \quad (37)$$

A paradoxical feature of this source function is that the information about the velocity v of the pair's center-of-mass frame with respect to the source has disappeared. Thus, we have the same source function in the source rest frame and in the center-of-mass frame of the pair. However, when we transform the correlation function from the pair center-of-mass to the source rest frame the pair velocity enters. The advantage of Eq. (37) is that the calculations can be performed almost analytically.

Substituting the source function (37) into Eq. (24), one finds

$$C(q_x^*, 0, 0) = \frac{2G(q_x^*)}{\sqrt{\pi}R_z} \int_0^\infty dz |{}_1F_1(-i\frac{\eta}{q_x^*}, 1, iq_x^*z)|^2 e^{-\frac{z^2}{4R_z^2}} , \quad (38)$$

$$C(0, q_y^*, 0) = \frac{2G(q_y^*)}{\sqrt{\pi}R_z} \int_0^\infty dz |{}_1F_1(-i\frac{\eta}{q_y^*}, 1, iq_y^*z)|^2 e^{-\frac{z^2}{4R_z^2}} , \quad (39)$$

$$\begin{aligned} C(0, 0, q_z^*) &= \frac{G(q_z^*)}{2\sqrt{\pi}R_z} \int_0^\infty dz |{}_1F_1(-i\frac{\eta}{q_z^*}, 1, 2iq_z^*z)|^2 e^{-\frac{z^2}{4R_z^2}} \\ &\quad + 2 \int_0^\infty dz \left[\operatorname{Re} \left(e^{-2iq_z^*z} {}_1F_1(-i\frac{\eta}{q_z^*}, 1, 2iq_z^*z) \right) + 1 \right] e^{-\frac{z^2}{4R_z^2}} . \end{aligned} \quad (40)$$

For pions the integration over z is performed using the approximate expression of the hypergeometric confluent function (B9). Thus, we find

$$C(q_x^*, 0, 0) = 2G(q_x^*) \left[1 + \frac{4\eta R_z}{\sqrt{\pi}} {}_2F_2\left(\frac{1}{2}, 1; \frac{3}{2}, \frac{3}{2}; -4q_x^{*2}R_z^2\right) \right] ,$$

$$C(0, q_y^*, 0) = 2G(q_y^*) \left[1 + \frac{4\eta R_z}{\sqrt{\pi}} {}_2F_2\left(\frac{1}{2}, 1; \frac{3}{2}, \frac{3}{2}; -4q_y^{*2}R_z^2\right) \right] ,$$

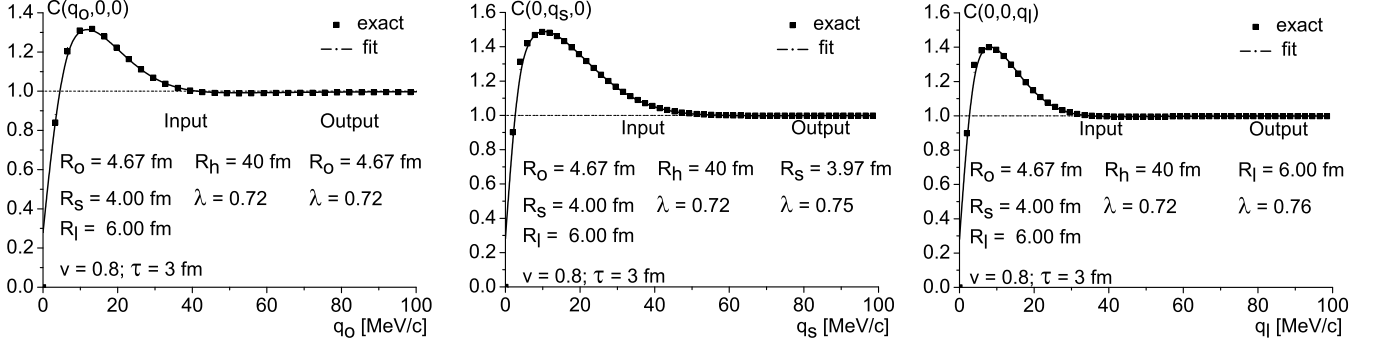


FIG. 12: The $\pi\pi$ Coulomb correlation functions $C(q_o, 0, 0)$ (left panel), $C(0, q_s, 0)$ (central panel) and $C(0, 0, q_l)$ (right panel) as functions of q_o , q_s or q_l , respectively. The fireball and halo parameters are $R_x = 4$ fm, $R_y = 4$ fm, $R_z = 6$ fm, $\tau = 3$ fm, $R_h = 40$ fm and the pair velocity is $\mathbf{v} = (0.8, 0, 0)$. The exact Coulomb correlation functions are shown with the squares and the Coulomb correlation functions fitted with the Bowler-Sinyukov formula (42) are represented by the solid lines.

$$\begin{aligned} C(0, 0, q_z^*) &= G(q_z^*) \left(1 + e^{-4q_z^{*2}R_z^2} \right) + G(q_z^*) \frac{4\eta R_z}{\sqrt{\pi}} {}_2F_2\left(\frac{1}{2}, 1; \frac{3}{2}, \frac{3}{2}; -4q_z^{*2}R_z^2\right) \\ &\times \left(1 + \sum_0^\infty (-1)^n \frac{(4q_z^* R_z)^{2n} n!} {(2n)!} \frac{{}_2F_2\left(\frac{1}{2}, n+1; \frac{3}{2}, \frac{3}{2}; -4q_z^{*2}R_z^2\right)} {{}_2F_2\left(\frac{1}{2}, 1; \frac{3}{2}, \frac{3}{2}; -4q_z^{*2}R_z^2\right)} \right). \end{aligned}$$

The Bowler-Sinyukov procedure works very well for the correlation function computed with the extremely anisotropic source function (37) with $R_z = 6$ fm. To make the test of the procedure even more challenging, we have considered an extremely anisotropic source of finite lifetime. The Coulomb correlation functions of pions and kaons, which are computed for the source of $R_x = R_y = 0$, $R_z = 6$ fm, $\tau = 3$ fm and $v = 0.8$, are shown in Fig. 9. The ‘free’ correlation functions, which are presented in Fig. 10, are obtained from the correlation functions shown in Fig. 9 by dividing them by the correction factor $K(q)$. The factor is computed for the averaged radius $R = \sqrt{(R_0^2 + R_l^2)/3}$. As seen, the Bowler-Sinyukov procedure works very well for both pions and kaons. In particular, $C_{\text{free}}(0, q_s, 0) = C(0, q_s, 0)/K(q) \approx 2$ as expected.

X. COULOMB CORRECTION WITH HALO

The procedure to eliminate the Coulomb interaction is more complex when the halo is taken into account. We test two versions of the procedure which, following the STAR Collaboration [13], we call the ‘dilution’ method and the ‘proper Bowler-Sinyukov’ one. The experimentally measured correlation functions $C(\mathbf{q})$ are fitted as

$$C(\mathbf{q}) = (1 - \lambda + \lambda K(q)) \left[1 + \lambda (C_{\text{free}}(\mathbf{q}) - 1) \right], \quad (41)$$

in the case of the dilution method and

$$C(\mathbf{q}) = 1 - \lambda + \lambda K(q) C_{\text{free}}(\mathbf{q}), \quad (42)$$

in the case of the Bowler-Sinyukov method.

The Coulomb correlation functions fitted according to the dilution (41) and Bowler-Sinyukov (42) formulas are shown in Fig. 11, 12, respectively. The source parameters are given in the figures. The *input* parameters are those used in the computation of Coulomb correlation functions: the fireball parameters are $R_x = 4$ fm, $R_y = 4$ fm, $R_z = 6$ fm and $\tau = 3$ fm; the halo is of zero lifetime of the radius $R_h = 40$ fm, and the pair velocity is $\mathbf{v} = (0.8, 0, 0)$. The *output* parameters are obtained from the fit. As seen, they only slightly deviate from the input parameters. Since the formulas (41, 42) do not work at $q \leq 1/R_h$, we perform the fit in the domain of q_o , q_s or q_l , respectively, bigger than 6 MeV. As seen the Coulomb correlation functions are fitted very accurately with both the dilution (41) and Bowler-Sinyukov (42) formulas.

The ‘free’ correlation functions extracted according to the dilution (41) and Bowler-Sinyukov (42) formulas are shown in Fig. 13, 14, respectively. The expected free functions are also shown for comparison. It is important to note that the parameter λ is assumed here to be known that is the actual value of λ enters the formula (41) or (42).

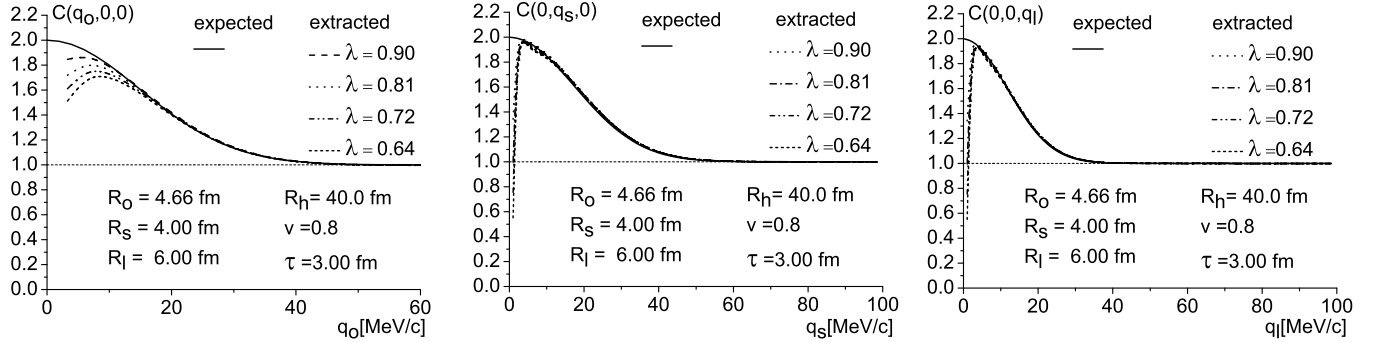


FIG. 13: The $\pi\pi$ free correlation functions $C(q_o, 0, 0)$ (left panel), $C(0, q_s, 0)$ (central panel) and $C(0, 0, q_l)$ (right panel) as functions of q_o , q_s or q_l , respectively. The fireball and halo parameters are $R_x = 4$ fm, $R_y = 4$ fm, $R_z = 6$ fm, $\tau = 3$ fm, $R_h = 40$ fm and the pair velocity is $v = (0.8, 0, 0)$. The ‘free’ correlation functions are extracted by means of the dilution method for several values of λ . The actual free correlation functions are shown by the solid lines.

As seen, the extracted correlation functions are distorted at small relative momenta and the distortions grow with λ . However, the widths of the correlation functions are unaltered and so are the source parameters.

The experimentally obtained ‘free’ functions, which are shown e.g. in Fig. 4 from [13], do not reveal the dip at small \mathbf{q} seen Fig. 13 and 14. We note, however, that the experimental correlations function in, say, out direction are not of the form $C(q_o, 0, 0)$ but rather $\int dq_s dq_l C(q_o, q_s, q_l)$ and the domain of truly small \mathbf{q} is not seen.

As mentioned at the end of Sec. VI, the model of halo should in principle include its finite lifetime. However, the finite lifetime increases the halo size in the out direction and the ‘free’ correlation function in out direction is distorted at even smaller momenta than the ‘free’ correlation functions in side and long directions. Therefore, our conclusions cannot be changed by taking into account a finite duration of pion emission from the halo.

XI. CONCLUSIONS

Let us summarize our study of the two-particle correlation functions. We have derived a relativistic generalization of the nonrelativistic Koonin formula. The calculations have been performed in the center-of-mass frame of the pair where a nonrelativistic wave function of the particle’s relative motion is meaningful. It required an explicit transformation of the source function to the center-of-mass frame of the pair. Finally, the correlation function has been transformed to the source rest frame as a Lorentz scalar field. The Coulomb correlation functions of pairs of identical pions and kaons have been computed. The source has been anisotropic and of finite lifetime. For pions the effect of halo has been also taken into account. The source function has been always of the Gaussian form.

Having the exact Coulomb correlation functions, the Bowler-Sinyukov procedure to remove Coulomb effect was tested. It was shown that the procedure works very well even for an extremely anisotropic source provided the halo is absent. For kaons small deviations are observed for a sufficiently large source. When the halo is included the pion correlation function are noticeably distorted for very small relative momenta but the source radii remain uninfluenced. Thus, we conclude that the Bowler-Sinyukov procedure, which at first glance does not look very reliable, appears to be surprisingly accurate. A possible interplay of Coulomb effects and fireball’s expansion has not been studied here but our analysis shows that Coulomb effects are not sensitive to the source’s shape as long as the characteristic source radius is much smaller than the Bohr radius of the particle’s pair of interest. Then, the Bowler-Sinyukov procedure is expected to work well.

APPENDIX A: DERIVATION OF CORRELATION FUNCTION

We sketch here the derivation, which is discussed in detail in [33, 34, 35], of the correlation function of two identical interacting bosons. Under rather general conditions, the correlation function as defined by Eq. (1) can be written down as

$$C(p_1, p_2) = \int d^4x_1 d^4x'_1 d^4x_2 d^4x'_2 \rho(x_1, x_2; x'_1, x'_2) \Psi_{p_1, p_2}(x_1, x_2) \Psi_{p_1, p_2}^*(x'_1, x'_2), \quad (\text{A1})$$

where $\rho(x_1, x_2; x'_1, x'_2)$ is the properly normalized coordinate space density matrix describing production process of the two particles and $\Psi_{p_1, p_2}(x_1, x_2)$ is the Bethe-Salpeter amplitude; $x_1, x_2, x'_1, x'_2, p_1, p_2$ are all four-vectors.

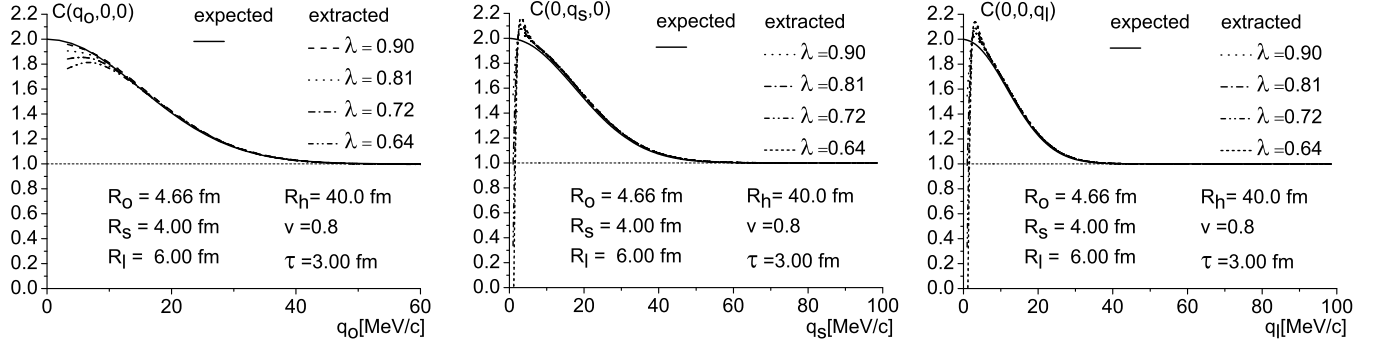


FIG. 14: The $\pi\pi$ ‘free’ correlation functions $C(q_0, 0, 0)$ (left panel), $C(0, q_s, 0)$ (central panel) and $C(0, 0, q_l)$ (right panel) as functions of q_0 , q_s or q_l , respectively. The fireball and halo parameters are $R_x = 4$ fm, $R_y = 4$ fm, $R_z = 6$ fm, $\tau = 3$ fm, $R_h = 40$ fm and the pair velocity is $\mathbf{v} = (0.8, 0, 0)$. The ‘free’ correlation functions are extracted by means of the Bowler-Sinyakov method for several values of λ . The actual free functions are shown by the solid lines.

To separate the relative from center-of-mass motion, one uses the variables (18) and expresses the Bethe-Salpeter amplitude as $\Psi_{p_1, p_2}(x_1, x_2) = e^{iP\cdot X}\psi_q(x)$. Then, the integrals over X and X' are performed and the formula (A1) changes into

$$C(P, q) = \int d^4x d^4x' \rho_P(x; x') \psi_q(x) \psi_q^*(x') . \quad (\text{A2})$$

And now one argues that the density matrix $\rho_P(x; x')$ can be approximated by the diagonal form

$$\rho_P(x; x') = D_r(x) \delta^{(4)}(x - x') , \quad (\text{A3})$$

where $D_r(x)$ is the relative source function of probabilistic interpretation. The nonrelativistic counterpart of $D_r(x)$ is given by Eq. (7). To justify the expression (A3) one assumes that the effect of particle production can be factorized from the final state interaction, as the production process occurs at a much larger energy-momentum scale than the process of final state interaction. Substituting the formula (A3) into Eq. (A2) one finds

$$C(P, q) = \int d^4x D_r(x) |\psi_q(x)|^2 . \quad (\text{A4})$$

When the Bethe-Salpeter amplitude $\psi_q(x)$ is transformed to the center-of-mass frame of the pair of particles, it can be replaced by the nonrelativistic function $\varphi_{\mathbf{q}_*}(\mathbf{r}_*)$ when t_* is assumed to vanish. Then, one reproduces our formula (23).

APPENDIX B: APPROXIMATION OF CONFLUENT HYPERGEOMETRIC FUNCTION

We derive here an approximate expression of the Coulomb scattering function which holds when the source size is much smaller than the Bohr radius of the two interacting particles. The confluent hypergeometric function ${}_1F_1(a, b; z)$, which gives the Coulomb scattering function, is defined as

$${}_1F_1(a, b; z) = 1 + \sum_{n=1}^{\infty} \frac{z^n}{n!} \prod_{k=0}^{n-1} \frac{a+k}{b+k} . \quad (\text{B1})$$

The Coulomb scattering function corresponds to the arguments $a = -i\eta/q$, $b = 1$ and $z = i(qr - \mathbf{qr})$. Introducing the parabolic coordinate ξ we have $q\xi = qr - \mathbf{qr}$ and thus,

$${}_1F_1\left(-\frac{i\eta}{q}, 1; iq\xi\right) = 1 + \sum_{n=1}^{\infty} \frac{(iq\xi)^n}{(n!)^2} \prod_{k=0}^{n-1} \left(-\frac{i\eta}{q} + k\right) . \quad (\text{B2})$$

To obtain the desired approximation we write down a few first terms of the series (B2) and we rearrange them as

$${}_1F_1\left(-\frac{i\eta}{q}, 1; iq\xi\right) = 1 + \frac{-\frac{i\eta}{q}iq\xi}{(1!)^2} + \frac{-\frac{i\eta}{q}(-\frac{i\eta}{q} + 1)(iq\xi)^2}{(2!)^2} + \frac{-\frac{i\eta}{q}(-\frac{i\eta}{q} + 1)(-\frac{i\eta}{q} + 2)(iq\xi)^3}{(3!)^2} + \dots$$

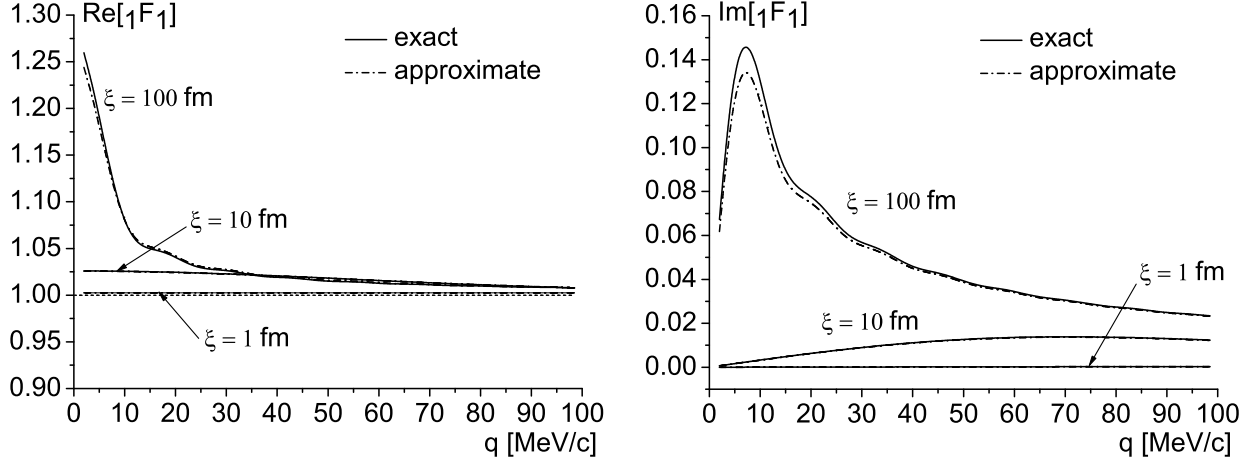


FIG. 15: The real (left panel) and imaginary (right panel) part of the pion Coulomb function ${}_1F_1(-i\eta_\pi/q, 1; iq\xi)$ as a function of q for several values of ξ . The solid and dashed lines represent, respectively, the exact formula (B2) and the approximation (B8).

$$\begin{aligned}
 &= 1 + \frac{\eta\xi}{(1!)^2} + \frac{\eta\xi(\eta\xi + iq\xi)}{(2!)^2} + \frac{\eta\xi(\eta\xi + iq\xi)(\eta\xi + 2iq\xi)}{(3!)^2} + \dots \\
 &= 1 + \sum_{n=1}^{\infty} \frac{1}{(n!)^2} \prod_{k=0}^{n-1} (\eta\xi + kiq\xi).
 \end{aligned} \tag{B3}$$

We first note that with the formula (B3), one easily finds the value of the Coulomb function at $q = 0$

$${}_1F_1\left(-\frac{i\eta}{q}, 1; iq\xi\right)\Big|_{q=0} = 1 + \sum_{n=1}^{\infty} \frac{1}{(n!)^2} \prod_{k=0}^{n-1} (\eta\xi) = \sum_{n=0}^{\infty} \frac{(\eta\xi)^n}{(n!)^2} = I_0(2\sqrt{\eta\xi}), \tag{B4}$$

where $I_v(z)$ is the modified Bessel function of the first kind defined as

$$I_v(z) = \sum_{k=0}^{\infty} \frac{1}{\Gamma(k+v+1)k!} \left(\frac{z}{2}\right)^{2k+v}.$$

We define the new variables $x \equiv \eta\xi$ and $y \equiv iq/\eta$, and we write down the series (B3) as

$${}_1F_1\left(\frac{1}{y}, 1; xy\right) = 1 + \underbrace{\frac{x}{(1!)^2}}_{n=1} + \underbrace{\frac{x^2(1+y)}{(2!)^2}}_{n=2} + \underbrace{\frac{x^3(1+y)(1+2y)}{(3!)^2}}_{n=3} + \dots \tag{B5}$$

We are interested in the approximation which holds when the source size is much smaller than the Bohr radius of the scattering particles that is when $x \ll 1$. Since y can be arbitrary big, the series cannot be simply terminated at a given power of x . Instead, one should take into account the lowest power of x for every power of y . For this purpose we have to rearrange the series (B5). After rather tedious analysis, one shows that

$${}_1F_1\left(\frac{1}{y}, 1; xy\right) = 1 + \sum_{k=0}^{\infty} y^k \sum_{n=k+1}^{\infty} \left(\sum_{l_1=1}^{n-k} \sum_{l_2=l_1+1}^{n-k+1} \dots \sum_{l_k=l_1+k-1}^{n-1} l_1 l_2 \dots l_k \right) \frac{x^n}{(n!)^2}. \tag{B6}$$

And now for each k in the series (B6) we take into account only the term of the lowest order of x that is we include only the term of $n = k + 1$. Observing that

$$\sum_{l_1=1}^1 \sum_{l_2=l_1+1}^2 \dots \sum_{l_k=l_1+k-1}^k l_1 l_2 \dots l_k = k!,$$

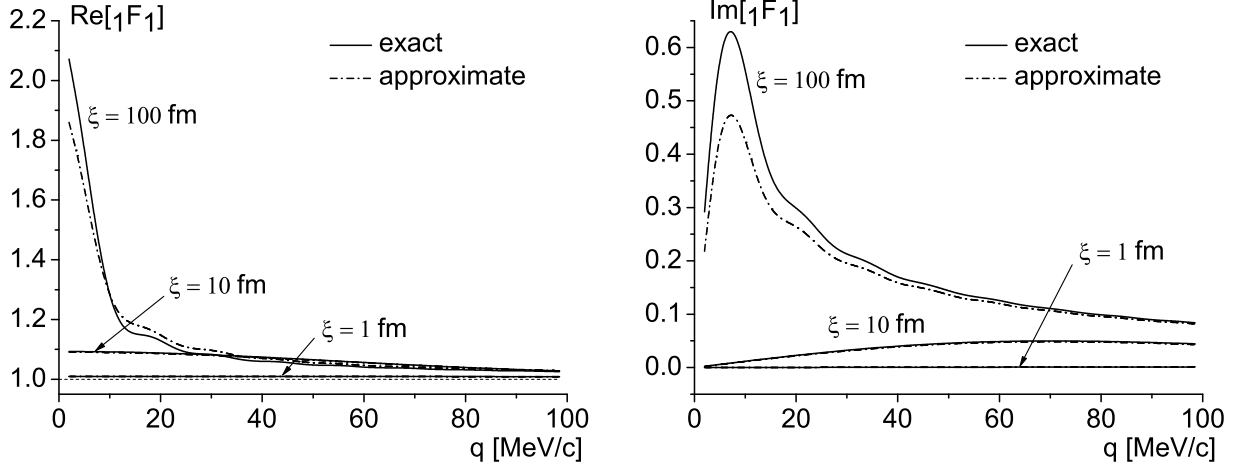


FIG. 16: The real (left panel) and imaginary (right panel) part of the kaon Coulomb function ${}_1F_1(-i\eta_K/q, 1; iq\xi)$ as a function of q for several values of ξ . The solid and dashed lines represent, respectively, the exact formula (B2) and the approximation (B8).

we obtain the desired approximation

$${}_1F_1\left(\frac{1}{y}, 1; xy\right) \approx 1 + \frac{1}{y} \sum_{k=0}^{\infty} \frac{(xy)^{k+1}}{(k+1)!(k+1)} = 1 + \frac{i}{y} \text{Si}(-ixy) - \frac{1}{y} (\gamma_e + \ln(-ixy) - \text{Ci}(-ixy)), \quad (\text{B7})$$

where $\text{Si}(z)$ and $\text{Ci}(z)$ are integral sine and cosine functions, respectively, and $\gamma_e \approx 0.5772$ is the Euler's constant. Reintroducing the physical arguments, we finally have

$${}_1F_1\left(-\frac{i\eta}{q}, 1; iq\xi\right) \approx 1 + \frac{\eta}{q} \text{Si}(q\xi) + i \frac{\eta}{q} (\gamma_e + \ln(q\xi) - \text{Ci}(q\xi)). \quad (\text{B8})$$

In Figs. 15 and 16 we show the Coulomb functions computed from the approximate formula (B8) for the Bohr radius of pions and kaons, respectively. As seen, the approximation works very well for pions ($\eta_\pi^{-1} = 388 \text{ fm}$) but it is not so accurate for kaons ($\eta_K^{-1} = 110 \text{ fm}$). We also see that $\text{Re}[{}_1F_1(-i\eta/q, 1; iq\xi)] \gg \text{Im}[{}_1F_1(-i\eta/q, 1; iq\xi)]$. Therefore, the imaginary part can be neglected and

$${}_1F_1\left(-\frac{i\eta}{q}, 1; iq\xi\right) \approx 1 + \frac{\eta}{q} \text{Si}(q\xi). \quad (\text{B9})$$

Since $\frac{\eta}{q} \text{Si}(q\xi) \ll 1$, we also have

$$\left| {}_1F_1\left(-\frac{i\eta}{q}, 1; iq\xi\right) \right|^2 \approx 1 + 2 \frac{\eta}{q} \text{Si}(q\xi). \quad (\text{B10})$$

The approximations (B9, B10) were used to compute the correlation functions of pions but not of kaons.

ACKNOWLEDGEMENTS

We are very grateful to W. Broniowski, W. Florkowski, A. Kisiel and R. Lednický for numerous fruitful discussions. This work was partially supported by Polish Ministry of Science and Higher Education under grant N202 080 32/1843.

-
- [1] U. A. Wiedemann and U. W. Heinz, Phys. Rept. **319**, 145 (1999).
 - [2] U. W. Heinz and B. V. Jacak, Ann. Rev. Nucl. Part. Sci. **49**, 529 (1999).
 - [3] M. A. Lisa, S. Pratt, R. Soltz and U. Wiedemann, Ann. Rev. Nucl. Part. Sci. **55**, 357 (2005).

- [4] Z. Chajecki, Acta Phys. Polon. B **40**, 1119 (2009).
- [5] M. G. Bowler, Phys. Lett. **B270**, 69 (1991).
- [6] Yu. Sinyukov, R. Lednický, S. V. Akkelin, J. Pluta and B. Erazmus, Phys. Lett. **B432**, 248 (1998).
- [7] C. Alt *et al.* [NA49 Collaboration], Phys. Rev. C **77**, 064908 (2008).
- [8] D. H. Rischke and M. Gyulassy, Nucl. Phys. **A597**, 701 (1996).
- [9] D. H. Rischke and M. Gyulassy, Nucl. Phys. **A608**, 479 (1996).
- [10] C. Adler *et al.* [STAR Collaboration], Phys. Rev. Lett. **87**, 082301 (2001).
- [11] K. Adcox *et al.* [PHENIX Collaboration], Phys. Rev. Lett. **88**, 192302 (2002).
- [12] S. S. Adler *et al.* [PHENIX Collaboration], Phys. Rev. Lett. **93**, 152302 (2004).
- [13] J. Adams *et al.* [STAR Collaboration], Phys. Rev. C **71**, 044906 (2005).
- [14] M. Gyulassy, Lect. Notes Phys. **583**, 37 (2002).
- [15] S. Pratt, Nucl. Phys. **A715**, 389 (2003).
- [16] D. A. Brown and P. Danielewicz, Phys. Lett. **B398**, 252 (1997).
- [17] D. A. Brown, A. Enokizono, M. Heffner, R. Soltz, P. Danielewicz and S. Pratt, Phys. Rev. C **72**, 054902 (2005).
- [18] S. Y. Panitkin *et al.* [E895 Collaboration], Phys. Rev. Lett. **87**, 112304 (2005).
- [19] P. Chung *et al.*, Phys. Rev. Lett. **91**, 162301 (2003).
- [20] S. S. Adler *et al.* [PHENIX Collaboration], Phys. Rev. Lett. **98**, 132301 (2007).
- [21] S. Afanasiev *et al.* [PHENIX Collaboration], Phys. Rev. Lett. **100**, 232301 (2008).
- [22] C. Alt *et al.* [NA49 Collaboration], [arXiv:nucl-ex/0809.1445].
- [23] W. Broniowski, M. Chojnacki, W. Florkowski and A. Kisiel, Phys. Rev. Lett. **101** (2008) 022301.
- [24] S. Pratt, Acta Phys. Polon. B **40**, 1249 (2009).
- [25] Yu. M. Sinyukov, A. N. Nazarenko and I. A. Karpenko, Acta Phys. Polon. B **40**, 1109 (2009).
- [26] C. Gombeaud, T. Lappi and J. Y. Ollitrault, Phys. Rev. C **79**, 054914 (2009).
- [27] R. Maj and St. Mrówczyński, Proceedings of XI International Workshop on Correlation and Fluctuation in Multiparticle Production, Hangzhou, China, November 21-25, 2006; Int. J. Mod. Phys. E **16**, 3244 (2007).
- [28] J. Adams *et al.* [STAR Collaboration], Phys. Rev. Lett. **93**, 012301 (2004).
- [29] M. A. Lisa [the STAR Collaboration], Acta Phys. Polon. B **35**, 37 (2004).
- [30] A. Kisiel, W. Florkowski, W. Broniowski and J. Pluta, Phys. Rev. C **73**, 064902 (2006).
- [31] S. Nickerson, T. Csorgo and D. Kiang, Phys. Rev. C **57**, 3251 (1998).
- [32] S. E. Koonin, Phys. Lett. **B70**, 43 (1977).
- [33] R. Lednický and V. L. Lyuboshits, Sov. J. Nucl. Phys. **35**, 770 (1982) [Yad. Fiz. **35**, 1316 (1981) (in Russian)].
- [34] R. Lednický and V. L. Lyuboshits, Heavy Ion Phys. **3**, 93 (1996).
- [35] R. Lednický, J. Phys. **G35**, 125109 (2008).
- [36] M. Jarvinen, Phys. Rev. D **71**, 085006 (2005).
- [37] S. Chapman, P. Scotto and U. W. Heinz, Phys. Rev. Lett. **74**, 4400 (1995).
- [38] U. Heinz, B. Tomasik, U. A. Wiedemann and Y. F. Wu, Phys. Lett. B **382** (1996) 181.
- [39] L.I. Schiff, *Quantum Mechanics* (McGraw-Hill, New York, 1968).
- [40] D. V. Anchishkin, W. A. Zajc and G. M. Zinovjev, Ukr. J. Phys. **41**, 363 (1996).
- [41] G. Bertsch, M. Gong and M. Tohyama, Phys. Rev. C **37**, 1896 (1988).
- [42] S. Pratt, Phys. Rev. D **33**, 1314 (1986).
- [43] G. Baym and P. Braun-Munzinger, Nucl. Phys. A **610**, 286C (1996).
- [44] U. A. Wiedemann and U. W. Heinz, Phys. Rev. C **56**, 3265 (1997).
- [45] We are very grateful to Richard Lednický for calling our attention to the fact that $q_0 = \mathbf{qv}$ not only for small \mathbf{q} , as we erroneously thought, but for any \mathbf{q} .